Self-Injection Locking and Phase-Locked States in Microresonator-Based Optical Frequency Combs

Pascal Del'Haye,* Katja Beha, Scott B. Papp, and Scott A. Diddams
National Institute of Standards and Technology (NIST), Boulder, Colorado 80305, USA
(Received 12 July 2013; published 29 January 2014)

Microresonator-based optical frequency combs have been a topic of extensive research during the last few years. Several theoretical models for the comb generation have been proposed; however, they do not comprehensively address experimental results that show a variety of independent comb generation mechanisms. Here, we present frequency-domain experiments that illuminate the transition of microcombs into phase-locked states, which show characteristics of injection locking between ensembles of comb modes. In addition, we demonstrate the existence of equidistant optical frequency combs that are phase stable but have nondeterministic phase relationships between individual comb modes.

DOI: 10.1103/PhysRevLett.112.043905 PACS numbers: 42.65.-k, 06.20.-f, 42.55.Sa, 42.65.Hw

Introduction.—Optical frequency combs have been a transformational physical measurement tool since their inception more than a decade ago [1,2]. As a ruler for optical frequencies, they enable precision measurements in the fields of optical clocks [3,4], astrophysical spectrometer calibration [5], and spectroscopy [6-8]. On the applied side, optical frequency combs are promising tools for multichannel generators in telecommunications [9,10], gas sensing [11], as optical and microwave frequency references [12], and for arbitrary optical waveform generation [13,14]. To date most optical frequency combs are based on femtosecond mode-locked lasers [2]. However, during the past five years a novel type of comb generator [15–35] has sparked significant scientific interest in new techniques and expanding applications of optical comb generation. The new comb generation principle is based on parametric four-wave mixing in a monolithic high-Q microresonator and does not utilize conventional stimulated laser emission. However, in contrast to a mode-locked laser comb there is little consensus on possible mode-locking mechanisms (e.g., a saturable absorber) in microcombs, which could align the phases to generate ultrashort optical pulses. This is the case for both experimental research on microcombs and recent theoretical studies that focus on a better understanding of the actual comb generation principle [36–44]. In this work, we present an extensive frequency-domain analysis on the transition of microcombs into phase-locked states. We show the presence of a self-injection locking mechanism within the resonator that is mediated via the parametric gain and support our measurements with a model for self-injection locking of microcombs. In contrast to injection locking of mode-locked lasers [45,46], in which a pulsed laser synchronizes with an injected pulse train, both the injected and driven oscillator are generated in the same microresonator.

In addition, we present phase measurements of the comb modes and show the existence of phase stable microcombs with uniform mode spacing but a nondeterministic phase relationship between individual comb lines. In contrast to mode-locked lasers and recent observation of soliton generation in a microcomb [47], these measurements indicate the existence of phase-locked microcombs without a circulating high-peak power pulse and related mode-locking mechanisms.

Experimental setup.—For our experiments, the microcomb is generated from a tunable diode laser that is amplified and coupled via a tapered optical fiber into a whispering-gallery mode of a fused silica microrod resonator (diameter 2.6 mm, mode spacing ~25.6 GHz, loaded quality factor $Q = 1.85 \times 10^8$) [34,48]. When the laser is tuned into a cavity resonance from the blue side, the resonator locks itself thermally to the laser [49] and generates an optical frequency comb. For resonators like the one we employ, the dispersion [50] dictates that the parametric gain is maximized for modes that are not adjacent to the pump. Just above threshold, this can lead to bunched combs [Fig. 1(a)], with bunches having the same mode spacing but mutual offsets [41,51] [Fig. 1(b)]. These offsets depend on the dispersion of the different mode families and typical values range from a few hundred kilohertz up to ~100 MHz. The measured group velocity dispersion of the mode family used for comb generation in this work is $\beta_2 = -14.5$ (ps^2/km) (see the Supplemental Material [52] for details). The offsets represent a departure from the uniform nature of an ideal frequency comb; however, we observe that injection locking can occur as bunches begin to overlap, leading to an offset-free, continuous comb. Similar locking effects have already been indicated in microcombs by disappearing sidebands in the microwave mode spacing beat note of microcombs [28,51].

In order to analyze the phase-locking behavior of a microcomb system and confirm the existence of a uniform and continuous comb, we measure the frequencies of the microcomb modes relative to those of an established mode-locked laser comb [see Fig. 1(c)]. This is accomplished

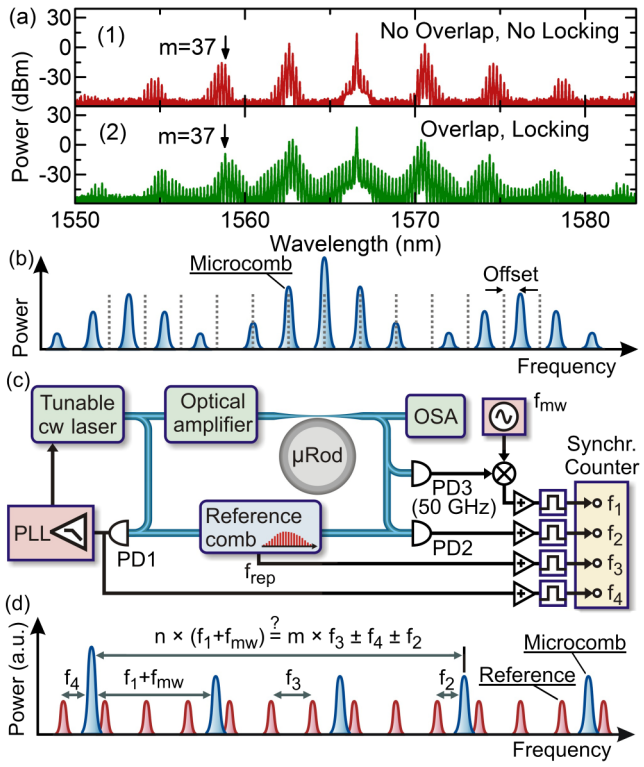

FIG. 1 (color online). (a) Optical spectra of microcombs without (1) and with (2) overlap. The amount of overlap can be controlled by changing the detuning of the pump laser with respect to the resonator mode. (b) Offset in a bunched microcomb. The dashed lines depict the position of equidistant comb modes. (c) Experimental setup to analyze and test self-injection-locking and phase-locking behavior of microcombs. OSA = optical spectrum analyzer, PLL = phase-locked loop, and PD = photodiode. (d) Scheme to determine whether the frequency of a comb mode is commensurate with that of a uniformly spaced comb.

with a multichannel synchronous phase and frequency recorder that measures the frequency spacing between the pump laser and nth comb sideband Δf_n as well as the microcomb's mode spacing f_{mc}. Any possible offset of the nth mode from its expected position is given as $f_{\mathrm{off}} = n \times f_{\mathrm{mc}} - \Delta f_n$. The microcomb spacing $f_{\mathrm{mc}} = f_{\mathrm{mw}} + f_1$ is measured by sending comb light onto a fast photodiode, mixing the signal down with a microwave reference f_{mw} and recording frequency f_1. The value $\Delta f_n = m \times f_3 \pm f_4 \pm f_2$ is measured with the reference comb by counting its repetition rate (f_3) as well as offset beat notes with the pump laser (f_4) and the nth microcomb sideband (f_2), respectively [cf. Fig. 1(d)]. In this way we obtain the offset as $f_{\mathrm{off}} = n \times (f_{\mathrm{mw}} + f_1) - m \times f_3 \pm f_4 \pm f_2$. The ambiguity of the $\pm$ signs in f_{off} can be resolved by slightly changing the offset of the reference comb and monitoring whether the beat frequencies f_2 and f_4 increase or decrease.

Injection locking.—The experimental setup in Fig. 1 allows us to monitor offsets in microcombs in real time. A microcomb is tuned into a state close to zero offset by changing the coupling to the resonator and the detuning between pump laser and resonator mode. Once in this state, the offset can be fine-tuned by slightly changing the power launched into the resonator [Fig. 2(a)]. Here, the x axis is offset by ~50 mW, which corresponds to the average launched power. It is observed that the measured offset locks to zero in a characteristic way that is known from injection locking [53,54]. This locking behavior can be modeled from the Adler equation (1) that describes the phase evolution for an injection-locked signal. In contrast to externally driven injection locking of conventional mode-locked lasers [45,46], in which all comb modes of injected and free running laser require a sufficient overlap, the self-injection locking in microresonators takes places in the region were two microcomb bunches start to overlap. This permits the use of a simple injection-locking model with only one free running and one injected frequency (see also the Supplemental Material [52]),

$$\frac{1}{2\pi}\frac{d\varphi(t)}{dt} = \Delta v - \frac{v_0}{2Q}\frac{E_1}{E_0}\sin\varphi(t). \tag{1}$$

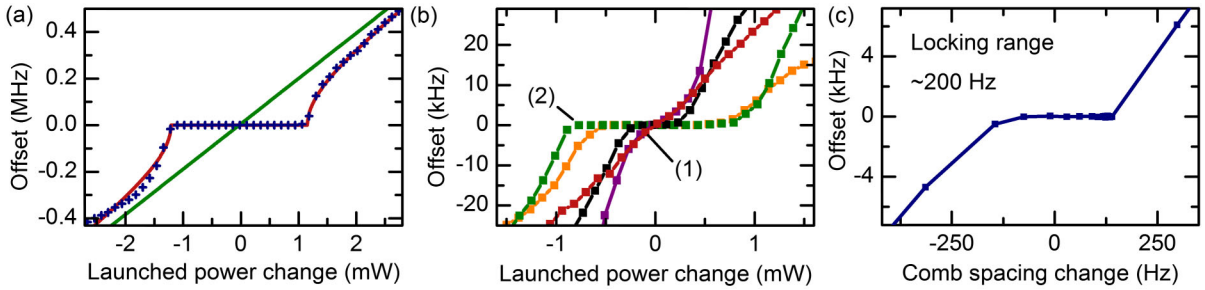

FIG. 2 (color online). Injection locking of bunched comb states. (a) Measured offset of the 37th sideband of a bunched microcomb (blue crosses) showing a characteristic injection-locking behavior. The red line is a fit based on the Adler equation. The green line going through the origin of the graph is obtained from the fit and shows how the offset would tune without injection locking present. Panel (b) shows the injection-locking behavior for different comb states with different overlap between bunches. Trace (1) shows a comb state without overlap between bunches, which shows no injection locking. Trace (2) shows a state with strong overlap that leads to injection locking. Corresponding optical spectra are shown in Fig. 1(a). Panel (c) shows the injection-locking range as function of the microcomb spacing (tuned via launched power).

Here, $v_0 \approx 193$ THz is the oscillator's free-running frequency, $Q = 1.85 \times 10^8$ is the loaded quality factor of the resonator, and E_1/E_0 is the relative field amplitude of the injected and free-running frequencies (in the case of a microcomb, this corresponds to the combined relative amplitudes of the comb modes in the regions of overlapping bunches). The variable $\Delta v = v_0 - v_1$ corresponds to the difference between injected frequency v_1 and free-running oscillator frequency v_0. In other words, Δv is the offset in a hypothetical microcomb without locking mechanism. In the case of self-injection locking of a microcomb, v_0 and v_1 are not directly accessible; however, the difference Δv tunes linearly with the launched power change ΔP such that $\Delta v = \kappa \Delta P$, with κ being a constant.

The solutions of the Adler equation (1) are periodic waveforms with an average frequency given by (cf. Ref. [53])

$$f_{\text{off}} = \left\langle \frac{d\phi(t)}{dt} \right\rangle = \Delta v \frac{\sqrt{K^2 - 1}}{|K|} = \kappa \Delta P \frac{\sqrt{K^2 - 1}}{|K|}, \quad (2)$$

with

$$K = 2Q \frac{E_0}{E_1} \frac{\kappa \Delta P}{v_0}. \quad (3)$$

A fit of the data in Fig. 2(a) using Eq. (2) shows excellent agreement with the injection-locking model. The only free parameters for the fit are $\kappa = (195 \pm 2)$ (kHz/mW) and the ratio $E_0/E_1 = 2.27 \pm 0.03$ [corresponding to a power ratio of $P_0/P_1 = (E_0/E_1)^2 = 5.2 \pm 0.1$]. The parameter κ corresponds to the offset tuning for large $|\Delta P|$ such that $|K| \gg 1$ (zero coupling between bunches). In this case the last term $(\sqrt{K^2 - 1}/|K|)$ in Eq. (2) approaches unity and $f_{\text{off}} \approx \Delta v = \kappa \Delta P$ [green line through the graph's origin in Fig. 2(a)]. The microcomb self-injection locks for $K^2 \leq 1$, leading to a locking range of

$$\Delta v_{\text{lock}} = \kappa \Delta P_{\text{lock}} = \frac{v_0}{Q} \frac{E_1}{E_0}. \quad (4)$$

In this range, the real part of f_{off} vanishes, leaving only an imaginary part. This imaginary part corresponds to a phase shift $\Delta\phi$ between the (self-)injected frequency v_1 and f_{off} with $-(\pi/2) < \Delta\phi < +(\pi/2)$. The other fitting parameter from Eqs. (2) and (3) is the ratio E_0/E_1, which determines the width of the locking range. Using Eq. (4) we obtain $\Delta v_{\text{lock}} = (460 \pm 6)$ kHz for the locking range obtained from the microcomb data of Fig. 2(a).

The importance of the overlap between bunches for self-injection locking is shown in Fig. 2(b). No locking behavior is observed when the microcomb bunches are far from overlapped [trace (1) in Fig. 2(b) with corresponding optical spectrum in Fig. 1(a)]. The amount of overlap between the comb bunches is controlled by changing the detuning of the pump laser frequency with respect to the microresonator mode. Figure 2(c) shows the measured offset as a function of the comb spacing change. As before, the comb spacing is changed by tuning the launched power. We can see that the microcomb spacing is more stable within the injection-locked range and tunes by only ~200 Hz. The measurement shows that the offset of the bunches (and thus the 37th sideband) tunes faster with launched power than the expected 37x "comb spacing," which facilitates the transition into the injection-locked state. A likely explanation for the different tuning is the power dependent shift of the parametric gain maximum.

Abruptly phase-locked combs.—In the same resonator mode, but at smaller detunings of the pump laser with respect to the microresonator mode (see the Supplemental Material [52] Fig. S4 for details), we observe another phase-locking behavior that has some different characteristics compared to the self-injection locking. In this case, we cannot tune continuously into the locked state, but the resonator rather abruptly transitions into a stable comb state with a characteristic and symmetric shape of the optical spectrum and low noise in the mode spacing beat note signal. Similar looking comb states have been observed in recent microcomb work [28,47,35]. One example of these comb states is shown in Fig. 3(a). The setup shown in Fig. 1(c) is used to determine whether the spectrum in Fig. 3(a) constitutes a continuous optical frequency comb without offsets. An optical filter is used in this measurement in order to count the offset of single comb sidebands. Figure 3(b) shows the result of an offset measurement for the 98th sideband of the microcomb. The offset shows a measurement time limited mean value of 740 μHz $\pm$ 3 mHz. Several comb modes [marked with arrows in Fig. 3(a)] have been measured and all of them reveal an offset consistent with zero. Figure 3(d) is the Allan deviation for offset measurements of the 98th and 37th sideband. These data show that the measured offset averages down to a few millihertz at 1000 seconds measurement time.

Further confirmation of the offset-free nature of this microcomb is shown in Fig. 3(e) where we observe the correlation between the microcomb mode spacing f_{mc} and the frequencies of the 37th, 61st, and 98th microcomb modes. The measurements show that the measured sidebands tune exactly as expected as $n \times f_{\text{mc}}$ (with n being the sideband number). Linear fits of the data in Fig. 3(e) (dotted lines) yield slopes of 97.995 ± 0.004, 60.99 ± 0.02, and 36.9998 ± 0.0004 for the 98th, 61st, and 37th sideband, respectively (with the uncertainty limited by the relatively short measurement time).

It is interesting to note that the phase-locked comb states shown in Fig. 3 are remarkably stable and can run continuously for several days. This stability permits more extensive measurements of the relative phases of the microcomb modes. In order to measure the phases of comb modes, we implement a liquid-crystal-based programmable

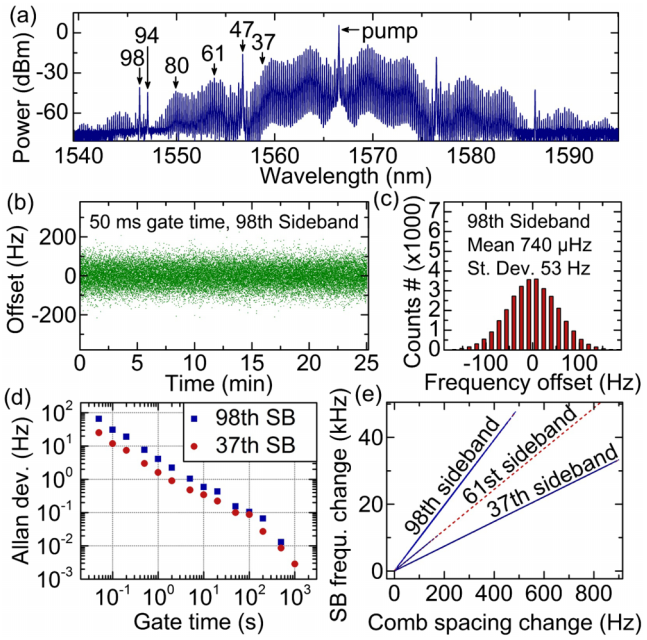

FIG. 3 (color online). (a) Optical spectrum of a phase-locked microresonator comb. (b) Measurement of the offset of the +98th comb sideband in a phase-locked state. The mean value of the measurement is 740 μHz $\pm$ 3 mHz. (c) Distribution of the data in panel (b). (d) Allan deviation (not normalized) of the offset of the +37th and +98th comb sideband. (e) Tuning of the 37th, 61st, and 98th sideband versus the measured comb spacing.

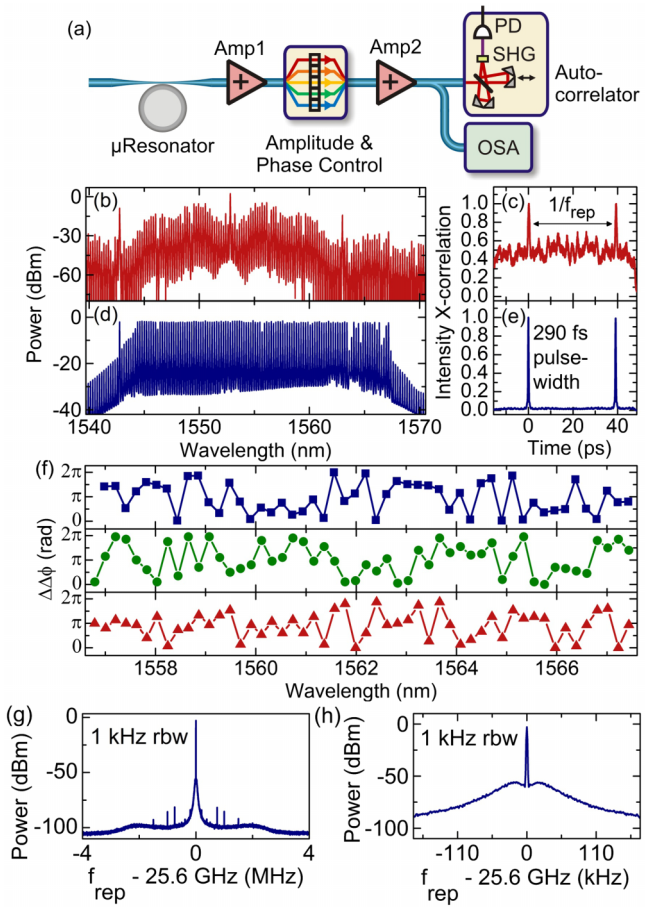

FIG. 4 (color online). Phase measurement of microresonator modes via optical autocorrelation. (a) Experimental setup. (b),(c) Optical spectrum and autocorrelation without amplitude and phase adjustments. (d),(e) Spectrum and autocorrelation after phase adjustment. (f) Second-order dispersion of the phases of three different phase-locked states. The phases of the comb modes in all three states appear to be random and unique but are stable in time. (g),(h) Mode spacing beat note of a phase-optimized microcomb at different scales.

"wave shaper" that enables control of the phases and amplitudes of individual microcomb modes. In conjunction with a nonlinear optical autocorrelator, this allows us to phase align all the microcomb modes such that they generate a short pulse [14,22]. Subsequently, we use this same control and measurement capability to infer the phase relationship among the modes within the microresonator. Note that by phase we mean the phase offset ϕ_n and not the time evolving instantaneous phase $(\omega_n t + \phi_n)$ of the nth comb mode. The experimental setup for the phase and amplitude control is shown in Fig. 4(a). Figures 4(b) and 4(c) show optical spectrum and autocorrelation of a phase-locked comb state without any phase adjustments. The autocorrelation has a background-to-peak ratio of ~0.5, which is characteristic for a comb spectrum with randomly distributed phase offsets. Figures 4(d) and 4(e) show the spectrum and autocorrelation after amplitude flattening and phase optimization. The pulse length determined from the autocorrelation is ~290 fs assuming a sinc-pulse shape (which is expected from a rectangular shaped optical spectrum). The same transform limited pulse length is obtained from a calculated pulse with the spectral amplitudes of the comb modes in Fig. 4(d).

Knowledge of the phases that have been applied to the comb modes to generate a short pulse combined with the additional measurement of the setup dispersion allows us to calculate the phases of the modes at the point where the comb exits the resonator. It is important to know that the resulting pulse envelope is independent of a constant offset of all phases and also independent of a linear increase in phase with frequency (the latter just shifts the pulse in time). Thus, in order to eliminate linear phase changes, we analyze the second derivative of the phases, which we define as the phase dispersion

$$\Delta\Delta\phi \equiv \phi_{n+1} + \phi_{n-1} - 2\phi_n. \quad (5)$$

In case of quadratic dispersion in the comb modes, $\Delta\Delta\phi$ is expected to be constant. Taking third-order dispersion into account, $\Delta\Delta\phi$ would vary linearly. Figure 4(f) shows measurements of $\Delta\Delta\phi$ for three different phase-locked comb states that have been transformed into transform limited pulses. We find that there is no evident pattern in the distribution of $\Delta\Delta\phi$ and a different phase dispersion for all measured phase-locked states. Running the phase retrieval

twice for the same phase-locked state returns the same distribution for $\Delta\Delta\phi$ with a mean absolute deviation of $\sim 2\pi/13$ rad, which is a good estimate for the error on the phase measurement. Together with the data in Fig. 3, this measurement indicates the existence of stable phase-locked microcomb states with nondeterministic phase distributions among the comb modes.

Figures 4(g) and 4(h) show the mode spacing beat note of an amplitude- and phase-optimized frequency comb at ~25.6 GHz. The signal-to-noise ratio of more than 100 dB in 1 kHz resolution bandwidth is further evidence of stable phase-locked operation.

Summary.—We have shown the existence of self-injection locking of optical frequency combs in microresonators. Even though the injection locking takes place simultaneously between many different comb modes, it is possible to describe the process as a simple two-frequency injection-locking mechanism. Moreover, we have analyzed intrinsically phase-locked states in a microresonator with apparently disorganized but stable phases in time. These results imply that injection locking between multiple parametric processes can play an important role in stable parametric comb generation. Additionally, our results demonstrate the existence of frequency comb generation in microresonators that does not involve mode-locking mechanisms favoring high-peak power. This is a surprising departure from the processes required in conventional mode-locked lasers. Moreover, we have shown that the generated combs are long-term phase stable and can be transformed into short pulses, which is an important prerequisite for spectral broadening and self-referencing. In future research it will be important to understand how the presented self-injection-locked and phase-locked states are related and whether there is a connection to previously reported time-domain soliton generation [47,35] in microresonator-based optical frequency combs.

This work is supported by NIST, the DARPA QuASAR program, AFOSR, and NASA. P. D. thanks the Humboldt Foundation for support. We further thank Frank Quinlan and Jeff Sherman for helpful comments on the manuscript. This Letter is a contribution of NIST and is not subject to copyright in the United States.

*pascal.delhaye@gmx.de

[1] T. W. Hansch, Rev. Mod. Phys. **78**, 1297 (2006).
[2] S. T. Cundiff and J. Ye, Rev. Mod. Phys. **75**, 325 (2003).
[3] S. A. Diddams, T. Udem, J. C. Bergquist, E. A. Curtis, R. E. Drullinger, L. Hollberg, W. M. Itano, W. D. Lee, C. W. Oates, K. R. Vogel, and D. J. Wineland, Science **293**, 825 (2001).
[4] T. Rosenband, D. B. Hume, P. O. Schmidt, C. W. Chou, A. Brusch, L. Lorini, W. H. Oskay, R. E. Drullinger, T. M. Fortier, J. E. Stalnaker, S. A. Diddams, W. C. Swann, N. R. Newbury, W. M. Itano, D. J. Wineland, and J. C. Bergquist, Science **319**, 1808 (2008).
[5] T. Steinmetz, T. Wilken, C. Araujo-Hauck, R. Holzwarth, T. W. Hansch, L. Pasquini, A. Manescau, S. D'Odorico, M. T. Murphy, T. Kentischer, W. Schmidt, and T. Udem, Science **321**, 1335 (2008).
[6] F. Keilmann, C. Gohle, and R. Holzwarth, Opt. Lett. **29**, 1542 (2004).
[7] I. Coddington, W. C. Swann, and N. R. Newbury, Phys. Rev. Lett. **100**, 013902 (2008).
[8] B. Bernhardt, A. Ozawa, P. Jacquet, M. Jacquey, Y. Kobayashi, T. Udem, R. Holzwarth, G. Guelachvili, T. W. Hansch, and N. Picque, Nat. Photonics **4**, 55 (2009).
[9] P. J. Delfyett, S. Gee, M. T. Choi, H. Izadpanah, W. Lee, S. Ozharar, F. Quinlan, and T. Yilmaz, J. Lightwave Technol. **24**, 2701 (2006).
[10] J. S. Levy, A. Gondarenko, M. A. Foster, A. C. Turner-Foster, A. L. Gaeta, and M. Lipson, Nat. Photonics **4**, 37 (2009).
[11] S. A. Diddams, L. Hollberg, and V. Mbele, Nature (London) **445**, 627 (2007).
[12] T. M. Fortier, M. S. Kirchner, F. Quinlan, J. Taylor, J. C. Bergquist, T. Rosenband, N. Lemke, A. Ludlow, Y. Jiang, C. W. Oates, and S. A. Diddams, Nat. Photonics **5**, 425 (2011).
[13] Z. Jiang, C. B. Huang, D. E. Leaird, and A. M. Weiner, Nat. Photonics **1**, 463 (2007).
[14] F. Ferdous, H. X. Miao, D. E. Leaird, K. Srinivasan, J. Wang, L. Chen, L. T. Varghese, and A. M. Weiner, Nat. Photonics **5**, 770 (2011).
[15] P. Del'Haye, A. Schliesser, O. Arcizet, T. Wilken, R. Holzwarth, and T. J. Kippenberg, Nature (London), **450**, 1214 (2007).
[16] P. Del'Haye, O. Arcizet, A. Schliesser, R. Holzwarth, and T. J. Kippenberg, Phys. Rev. Lett. **101**, 053903 (2008).
[17] I. S. Grudinin, N. Yu, and L. Maleki, Opt. Lett. **34**, 878 (2009).
[18] D. V. Strekalov and N. Yu, Phys. Rev. A, **79**, 041805 (2009).
[19] T. J. Kippenberg, R. Holzwarth, and S. A. Diddams, Science **332**, 555 (2011).
[20] L. Razzari, D. Duchesne, M. Ferrera, R. Morandotti, S. Chu, B. E. Little, and D. J. Moss, Nat. Photonics **4**, 41 (2009).
[21] M. A. Foster, J. S. Levy, O. Kuzucu, K. Saha, M. Lipson, and A. L. Gaeta, Opt. Express **19**, 14233 (2011).
[22] Scott B. Papp and Scott A. Diddams, Phys. Rev. A **84**, 053833 (2011).
[23] P. Del'Haye, T. Herr, E. Gavartin, M. L. Gorodetsky, R. Holzwarth, and T. J. Kippenberg, Phys. Rev. Lett. **107**, 063901 (2011).
[24] Y. Okawachi, K. Saha, J. S. Levy, Y. H. Wen, M. Lipson, and A. L. Gaeta, Opt. Lett. **36**, 3398 (2011).
[25] I. S. Grudinin, L. Baumgartel, and N. Yu, Opt. Express **20**, 6604 (2012).
[26] A. R. Johnson, Y. Okawachi, J. S. Levy, J. Cardenas, K. Saha, M. Lipson, and A. L. Gaeta, Opt. Lett. **37**, 875 (2012).
[27] F. Ferdous, H. X. Miao, P. H. Wang, D. E. Leaird, K. Srinivasan, L. Chen, V. Aksyuk, and A. M. Weiner, Opt. Express **20**, 21033 (2012).
[28] J. Li, H. Lee, T. Chen, and K. J. Vahala, Phys. Rev. Lett. **109**, 233901 (2012).
[29] A. A. Savchenkov, A. B. Matsko, W. Liang, V. S. Ilchenko, D. Seidel, and L. Maleki, Phys. Rev. A **86**, 013838 (2012).
[30] A. A. Savchenkov, A. B. Matsko, W. Liang, V. S. Ilchenko, D. Seidel, and L. Maleki, Opt. Express **20**, 27290 (2012).

[31] P. H. Wang, F. Ferdous, H. X. Miao, J. Wang, D. E. Leaird, K. Srinivasan, L. Chen, V. Aksyuk, and A. M. Weiner, Opt. Express **20**, 29284(2012).
[32] A. Pasquazi, M. Peccianti, B. E. Little, S. T. Chu, D. J. Moss, and R. Morandotti, Opt. Express **20**, 27355 (2012).
[33] M. Peccianti, A. Pasquazi, Y. Park, B. E. Little, S. T. Chu, D. J. Moss, and R. Morandotti, Nat. Commun. **3**, 765 (2012).
[34] S. B. Papp, P. Del'Haye, and S. A. Diddams, Phys. Rev. X **3**, 031003 (2013).
[35] K. Saha, Y. Okawachi, B. Shim, J. S. Levy, R. Salem, A. R. Johnson, M. A. Foster, M. R. E. Lamont, M. Lipson, and A. L. Gaeta, Opt. Express **21**, 1335 (2013).
[36] Y. K. Chembo, D. V. Strekalov, and N. Yu, Phys. Rev. Lett. **104**, 103902 (2010).
[37] Y. K. Chembo and N. Yu, Opt. Lett. **35**, 2696 (2010).
[38] Y. K. Chembo and N. Yu, Phys. Rev. A **82**, 033801 (2010).
[39] A. B. Matsko, A. A. Savchenkov, V. S. Ilchenko, D. Seidel, and L. Maleki, Phys. Rev. A **85**, 023830 (2012).
[40] A. B. Matsko, A. A. Savchenkov, and L. Maleki, Opt. Lett. **37**, 4856 (2012).
[41] T. Herr, K. Hartinger, J. Riemensberger, C. Y. Wang, E. Gavartin, R. Holzwarth, M. L. Gorodetsky, and T. J. Kippenberg, Nat. Photonics **6**, 480 (2012).
[42] S. Coen, H. G. Randle, T. Sylvestre, and M. Erkintalo, Opt. Lett. **38**, 37 (2013).
[43] S. Coen, and M. Erkintalo, Opt. Lett. **38**, 1790 (2013).
[44] A. B. Matsko, W. Liang, A. A. Savchenkov, and L. Maleki, Opt. Lett. **38**, 525 (2013).
[45] M. Margalit, M. Orenstein, and H. A. Haus, IEEE J. Quantum Electron. **32**, 155 (1996).
[46] O. Gat and D. Kielpinski, New J. Phys. **15**, 033040 (2013).
[47] T. Herr, V. Brasch, J. D. Jost, C. Y. Wang, N. M. Kondratiev, M. L. Gorodetsky, and T. J. Kippenberg, arXiv:1211.0733 [Nat. Photon. (to be published)].
[48] P. Del'Haye, S. A. Diddams, and S. B. Papp, Appl. Phys. Lett. **102**, 221119 (2013).
[49] T. Carmon, L. Yang, and K. J. Vahala, Opt. Express **12**, 4742 (2004).
[50] P. Del'Haye, O. Arcizet, M. L. Gorodetsky, R. Holzwarth, and T. J. Kippenberg, Nat. Photonics **3**, 529 (2009).
[51] S. B. Papp, P. Del'Haye, and S. A. Diddams, Opt. Express **21**, 17615 (2013).
[52] See Supplemental Material at http://link.aps.org/supplemental/10.1103/PhysRevLett.112.043905 for details.
[53] R. Adler, Proc. IRE **34**, 351 (1946).
[54] A. E. Siegman, *Lasers* (University Science Books, Herndon, VA, 1986).